We are IntechOpen, the world's leading publisher of Open Access books Built by scientists, for scientists

6,900
Open access books available

185,000
International authors and editors

200M
Downloads

Our authors are among the

154
Countries delivered to

TOP 1%
most cited scientists

12.2%
Contributors from top 500 universities



WEB OF SCIENCE™

Selection of our books indexed in the Book Citation Index in Web of Science™ Core Collection (BKCI)

Interested in publishing with us?
Contact book.department@intechopen.com

Numbers displayed above are based on latest data collected.
For more information visit www.intechopen.com



Chapter 4

New Generation of Ultra-High Peak and Average Power Laser Systems

Vladimir Chvykov

Additional information is available at the end of the chapter

http://dx.doi.org/10.5772/intechopen.70720

Abstract

Ultra-high peak power laser systems are applicable in new and very promising areas, such as charged particles acceleration and inertial confinement of the fusion nuclear reaction. First one could be used as effective secondary source of Y and X-ray beams, which have multiple applications in industry and medicine if repetition rate will be increased, the last one could serve as a source of unlimited energy after transforming in to the power plants. New technologies are able to significantly increase the output peak power due to extraction of the higher energy extracting during pumping (EDP). The record of extracted energy about 200 J and output power of 5 PW were reached with this technique. Polarization Encoded Chirped Pulse Amplification (PE-CPA) technique as well as two stages of compression produced shorter pulse duration also are presented in this chapter. Besides, the capability of combination of the EDP method and the Thin Disk (EDP-TD) applied to Ti:Sa amplifiers to produce the higher repetition rate in the PW-class laser systems, as well as the results of the proof-of-principal experiments will be demonstrated.

Keywords: laser amplifiers, ultrafast lasers, lasers, titanium

1. Introduction

Ultra-high peak power laser pulses are the only way today to reach extremely high concentration of the energy in small volume after focusing with intensity 10^{22} W/cm^2 and above. This possibility makes the pulse laser systems as remarkable instruments for scientific research, if the high average power (high repetition rate) could be simultaneously reachable for industrial applications. The pulsed lasers require a much lower energy to get ultra-high powers comparing to continuous wave (CW)-regime. The situation became very promising when Q-switching [1] and mode-locking [2] regimes of laser operation were invented (**Figure 1**). This permitted to get a short enough laser pulse: nanosecond-level (10^{-9} s) at first and then consequently

IntechOpen

© 2018 The Author(s). Licensee IntechOpen. This chapter is distributed under the terms of the Creative Commons Attribution License (http://creativecommons.org/licenses/by/3.0), which permits unrestricted use, distribution, and reproduction in any medium, provided the original work is properly cited. CC BY

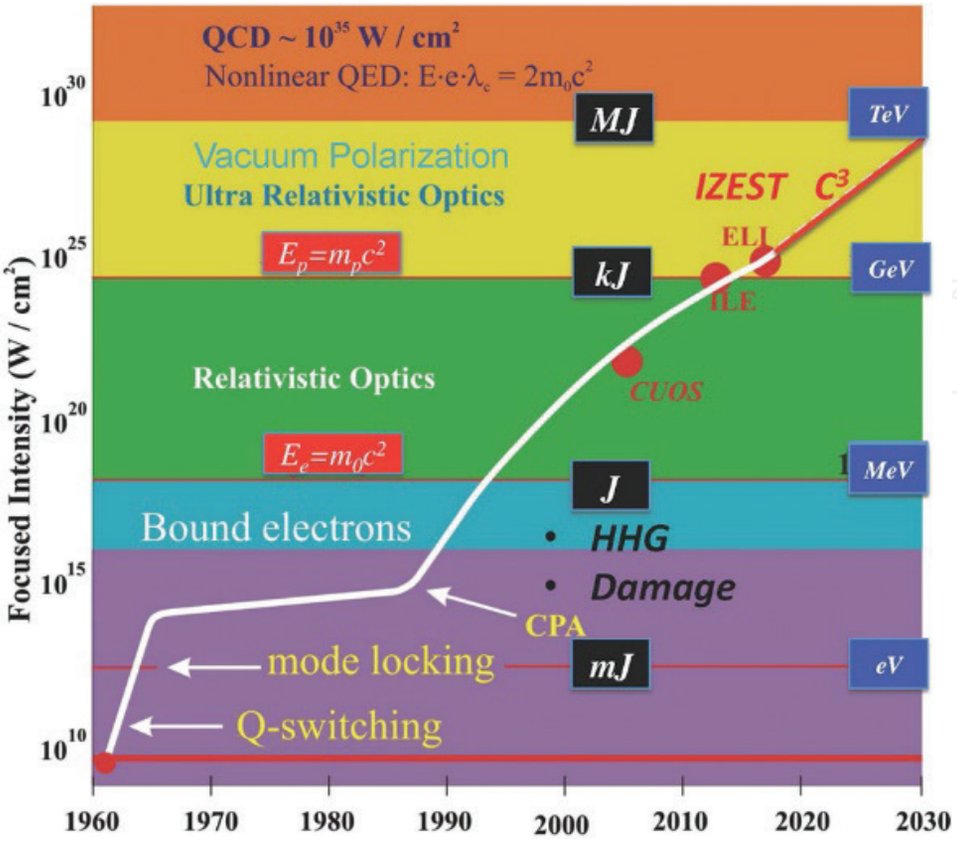


Figure 1. Intensity evolution since the first laser demonstration in 1960, with the different regimes of optics and electrodynamics. Black boxes (joules) indicate typical laser energies. Blue boxes (electron volts) indicate typical laser-plasma accelerated particle energies. (Courtesy G. Mourou.) http://www.spie.org/newsroom/4221-exploring-fundamental-physics-at-the-highest-intensity-laser-frontier?highlight=x2404&ArticleID=x88664&SSO=1 (QCD, quantum chromodynamics; QED, quantum electrodynamics; E, electric field; e, electron charge; λ_c, compton wavelength; m_0, electron mass; c, speed of light. E_p, proton energy; m_p, proton mass. E_e, electron energy; C^3, cascaded conversion compression; ELI, extreme light infrastructure; ILE, institut de la lumiere extreme; CUOS, Center for Ultrafast Optical Science University of Michigan; HHG, high harmonic generation; CPA, chirped pulse amplification).

picosecond (10^{-12} s) and femtosecond (10^{-15} s) pulse durations using mode-locking oscillators. The lasers based on these technologies, and applying also master oscillator power amplifier (MOPA) configuration, achieved MW and GW-levels of power or 10^{11}–10^{14} W/cm^2 after focusing. The ability to reach these high levels of power allowed to look forward to the application of these systems in other new and very promising areas, such as charged particles acceleration [3] and inertial confinement of the fusion nuclear reaction (ICF) [4]. The consequent evolution of these laser systems resulted in the tremendous National Ignition Facility (NIF) laser in the United States [5], and the Megajoule in Europe [6].

The prior, with its output energy in 192 laser beams about 4 MJ, is delivering to the target a power of up to 500 Terawatt. The laser occupies the area as large as three football fields (see **Figure 2a**) and consists of two laser bays, one of which is presented in **Figure 2b**.

So, a large area is required for these multichannel facilities due to damage threshold of the optical elements which is normally limited at 10 J/cm^2 for ns-scale of the pulse duration. Further increasing of the power is associated with unacceptable gigantism of the laser systems.

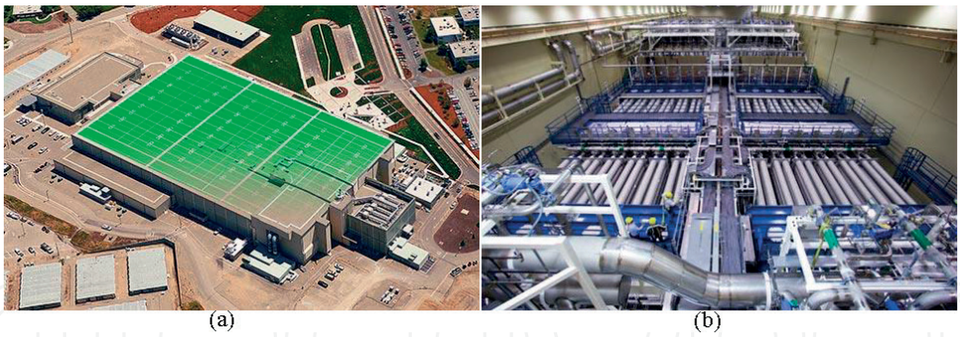


Figure 2. (a) NIF laser and target area building; (b) laser bay 2, one of NIF's two laser bays (from https://www.theguardian.com/environment/gallery/2009/may/28/national-ignition-facility-fusion-energy#img-7. http://archive.boston.com/bigpicture/2010/10/the_national_ignition_facility.html).

Nevertheless, the next multiorder step in increasing laser powers was done more than 20 years after the Q-switch invention, when chirped pulse amplification (CPA) technology was suggested in the mid-1980s and was related with significant reduction of the pulse duration for increasing peak power [7, 8] (**Figure 1**). The main goal of the CPA method is the reduction of optical elements and amplifier crystals size. If one will try to amplify the short laser pulse directly, undesirable nonlinear distortions of the pulse in the gain media and other optical elements will be reached very soon. This leads to self-focusing of the laser beam, and thus a growing intensity, which damages the optical elements. Therefore, one has to increase the beam diameter and the apertures of the amplifiers and others optics to avoid these problems. Nevertheless, the attempt to keep the intensity under the self-focusing threshold requires enormous apertures of the optical elements (e.g., several meters in diameter for petawatt output power).

Progressive idea of the CPA was adopted for the optical diapason and it gave an alternative way to increase pulse energy. Instead of enlarging the transverse beam size, increasing the pulse duration was suggested for further amplification, which was then followed by the pulse compression. Historically, first time, this idea was applied in the microwave diapason for radar technology in the 1960s. Soon, the stretching and compression of the laser pulse was suggested using different methods, among which were the use of compression in dispersive media [9], multilayer film interferometers [10] and, perhaps the most productive and widely explored today, the stretching and compression with a pair of diffraction gratings [11]. The first time when the pulse, chirped in a dispersive media (1.4 km of optical single mode fiber), was amplified and further compressed by a pair of diffraction gratings was done in 1985 [7, 8]. However, the distortion of the chirped pulse, introduced by the higher orders dispersion of the optical fiber made difficult to compensate by the grating compressor, and thus the output pulse duration was limited of a few picoseconds.

Most successful realization of this idea (Martínez-type stretcher setup containing a telescope between the gratings [12]) is presented in **Figure 3**, where the stretcher and compressor were both built on the base of diffraction gratings. The main clue can be explained very easily. Short pulse should possess a wide spectrum due to the Heisenberg uncertainty principle or other words, consist from the many harmonics. We can redirect different harmonics (parts) of this spectrum along different optical paths via diffraction, and thus get a different group

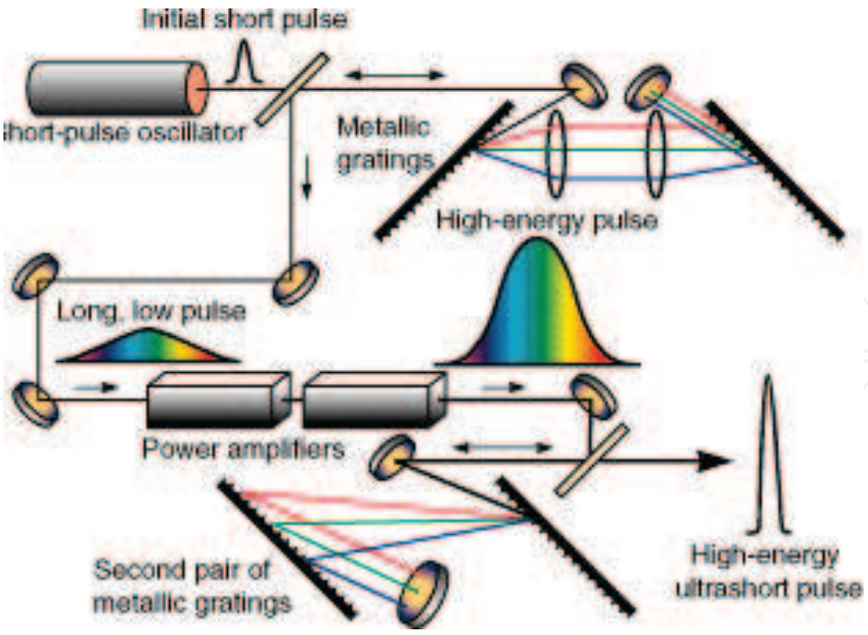


Figure 3. Simplified layout of the CPA laser system (from http://www.llnl.gov/str/Petawatt.html).

delay for each, finally guiding them consequently to the same direction and expanding such a way to the pulse duration. If in the stretcher, harmonics with longer wavelengths were directed along the shorter optical paths (positive or normal dispersion), then the compressor has to accomplish the reverse (negative or anomalous dispersion). Since the diffraction gratings are used both in the stretcher and the compressor, the functions of stretching and compression will be close to each other and the higher-order dispersion can be compensated up to 4th order.

Simplified layout of the classical CPA laser system is presented in **Figure 3**. Here the short pulse from the mode-locked oscillator passing through the stretcher is expanded usually by 4–5 orders. Further, the pulse with low intensity is amplified in the chain of amplifiers by several orders of magnitude, and is then compressed back to the short duration.

Several different laser active medias were used for oscillators and amplifiers in the CPA systems, such as dye, Nd:YAG, Nd:Glass, and so on. The most preferable from them was Ti:Sapphire (Ti:Sa) crystal due to its very large bandwidth emission spectra (FWHM ~ 200 nm), very high thermal conductivity and mechanical hardness. This setup was able to achieve pulse durations as short as below 10 femtosecond, if the Ti:Sa oscillators [13] with a few fs mode-locked pulse and amplifiers are adopted. Besides the laser amplifiers [14], optical parametrical amplifier (OPA) has been presented in CPA schemas [15].

Exploiting this technology, researchers developed laser systems with 100 s terawatt level output power and 10^{19} W/cm^2 intensity (see **Figure 1**) but, as any other technology, CPA has some boundaries on the continued improvement of its parameters, the foremost of which is the limitation on the output energy.

1.1. Limitation on the output energy

As mentioned above, CPA laser systems have reached sub-petawatt output powers with the energy as low as several tens of Joules [16]. However, for that new generation of the ultra-high power lasers, the modest energy will no longer be enough, and the kJ-level has to be reached setting the next milestone at tens or even hundreds of petawatt [17, 18]. The modern ability to stretch pulse duration is restricted at the few orders by the existing grating technology, so further energy increase requires once again the enlargement of amplifier apertures due to the damage threshold. There are two candidates for the final amplifier of the ultra-high CPA systems: the optical parametrical amplifiers [15] and the laser amplifiers. Both of them possess their own advantages and shortcomings. OPA has several attractive properties as the gain bandwidths large enough to support light pulses as shorter as 10 fs; low amplifier heating due to "Optical cooling," which leads to the potential of a high-repetition-rate; large high-quality nonlinear amplifier crystals; high pulse contrast due to the absence of amplified spontaneous emission (ASE) outside the pump pulse duration. At the same time, OPA possesses low efficiency (below 20%); there are severe requirements on the pump beam quality, such as limitation on the spatial fluctuations in amplitude; short pump pulses (below 1 ns), in order to match with the stretched signal pulses for higher efficiency and their precise matching in space and time with a ps accuracy; and so on [15].

The laser amplifiers are free of most of these restrictions, but possess problems of their own, which include severe losses due to th disk shape of the crystals and very high transverse gain and so the high transverse ASE (TASE), and possible parasitic generation (TPG). TASE as well as TPG leads to significant depletion of the inverted population, and thus the stored energy. The ASE from the pumped Ti:Sa crystal before and after the threshold of the parasitic generation is demonstrated in **Figure 4** [16]. The absence of ASE from the significant part of crystal demonstrates the reduction of the population inversion and so loses the stored energy. Because of this, enlarging the aperture of the amplifier fails to be an unlimited means of obtaining more output energy under the constraints imposed by the damage threshold limit. Therefore, in this case, the main limitation that arises on the path toward ultra-high output power and intensity is the restriction on the pumping and extraction energy imposed by

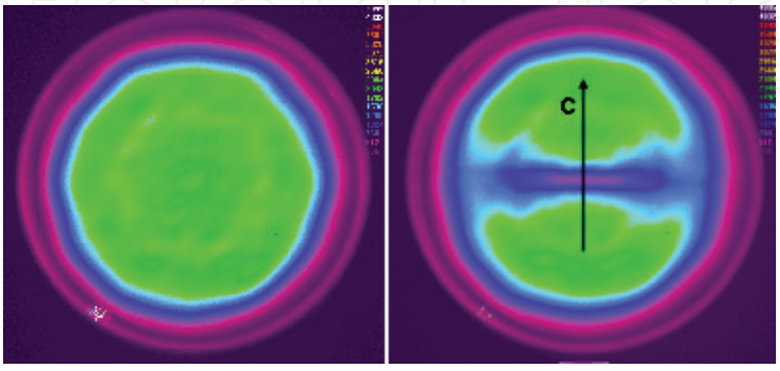


Figure 4. ASE from the pumped Ti:Sapphire crystal before and after threshold of parasitic generation [16].

TASE and TPG within the booster amplifier volume. As a result, the suppression of parasitic generation is a very important task that has been solved for the next generation of the ultra-high power laser systems. The technology allowed to solve this bottleneck problem will be discussed below in this chapter.

1.2. Gain narrowing during amplification

The making of the output short pulse shorter and keeping the same energy paved another way to the next milestone of the ultra-high peak power. Nevertheless, pulse duration of CPA lasers is strongly limited by gain narrowing of the pulse spectra in the gain medium of the multipass amplifiers (to around 30 fs of 100 TW–1 PW lasers based on Ti:Sa). Different approaches were entertained to overcome this limitation. Among them, there is a gain narrowing control by introduction of the thin film etalon into the front-end regenerative amplifier cavity. Impressive results were reached with this technique (pulse duration—16 fs with spectral width—72 nm) [19], but this method still suffers some restrictions, such as losses of the energy, a finite possibility of the broadening of the spectra due to the fluorescence spectrum limitation of the amplifier crystal, further gain narrowing in the buster and final amplifiers, as well as the limitation of the spectral transmission of the grating compressor.

The application of concept of optical-parametrical chirped pulse amplification (OPCPA) for broadband pulse allowed to reach a pulse duration of around 10 fs [20], but extremely severe requirements on the parameters of the pump laser which discussed above restrict output energy only to a few mJs. This way, an adequate method for shortening high-energy pulses has not yet been found. Two promising methods of the saving and restoring spectral bandwidth will be discussed also in this chapter.

1.3. Requirements for high repetition rate

With the light sources of 10–100 PW peak power, the accelerated electron beams can reach the energy up to TeV and ion beams up to GeV, (see **Figure 1**) as well as by using these secondary sources the ultra-bright X and Y-rays can be obtained [21]. These results could be widely applied into many areas of science, industry, medicine, homeland security, and so on. Nevertheless, it will be possible if the ultra-high peak power laser systems also will be able to combine with high repetition rate (hundreds of Hz to kHz) or high average power (kWs). In the petawatt class laser amplifiers, a pump pulse energy exceeds a few hundred J regime, which means significant thermal load in the gain medium even at low repetition rates.

Thin disk laser technology (TDT) is able to eliminate thermal distortions and damages of the laser crystals in the systems with both high peak and average output power [22]. However, conventionally used in TDT, Nd:YAG and Yb:YAG possess the narrow emission spectra and the low emission cross-section that lead to very complicated multipass amplification schemes which is practically acceptable only for low peak power systems with the ps-level pulse duration. The most promising crystal with required characteristics for ultra-high peak power laser is Ti:Sa, especially if one is taking into account its higher emission cross-section and thermal conductivity (compare 10 W/(mK) for YAG to 40 W/(mK) for sapphire at the room temperature and

more than two orders higher when cryogenically cooled). But the attempt to increase the longitudinal gain in TD-amplifier by rising the concentration of active ions and/or using crystals with higher emission cross-section leads to dramatic increase of the gain in the transverse direction and consequently to the big losses and inability to store pump energy due to TASE. Technology for solving this problem will be presented below in this chapter.

2. Extraction during pumping (EDP) method

As it was mentioned above, the main limitation that arises on the path toward ultra-high output power and intensity of the CPA laser systems is the restriction on the pumping and extraction energy imposed by TASE and TPG within the booster and final large aperture amplifier volume [23].

The reflectivity reduction of the side wall of the gain crystals by grinding, sandblasting and/or coating with an index-matched absorptive polymer or liquid layer in the laser amplifiers is the conventional procedure used to prevent parasitic generation (TPG) [24]. However, the difficulty to find the exact index matching within existing absorbers still restricts the diameter of the pump area to 6–8 cm, corresponding to an extracted energy to around 30 J from Ti:Sa [16]. The amplifier apertures enlarging, or to further pump fluence increasing has led to severe parasitic generation and has failed to increase extracted energy. The additional restriction on storing and extracting energy by TASE in larger gain apertures was demonstrated [25]. TASE necessarily increases with the aperture size, limiting the maximum stored energy that is why this restriction is even stronger than parasitic lasing because the threshold for the latter can be increased due to development of the new index matching materials for absorbers. The uniform luminescence on the left picture of **Figure 4** should not delude us, if one will find method to reduce reflections down to zero; the losses remain still incredible big for amplifiers with the large aperture.

The method of the calculation of total volume of TASE radiated out from the crystal during its pumping was developed by Chvykov et al. [25]. **Figure 5a** shows the evolution of normalized fluorescence of the crystals vs. pumping time when pumped by 100 ns-pulse for different crystal apertures. Here, E_{max} is the theoretical maximum of the extracted energy, and E_{loss} is the lost energy due to TASE. As seen from the plot, ASE grows dramatically after a certain time of pumping, even for 10 cm—crystal and soon becomes equal to the pumping energy. This means that further pumping is useless because all additional energy will be irradiated out of the crystal as ASE. The critical points of anomalous ASE (APs) are moving to the pumping process beginning with the growing crystal diameter. No more than 20–50% of the pump energy can be stored in the crystals with aperture of 15–20 cm as seen in **Figure 5**.

Shortening of the pump pulse duration does not help to reduce the losses, at least until pulse duration becomes shorter than the time-length of the light distribution through the crystal in transverse direction. This is about several 100 ps, and thus such a pump would be useless due to the very low damage threshold. Fluorescence during pumping for different pump pulse

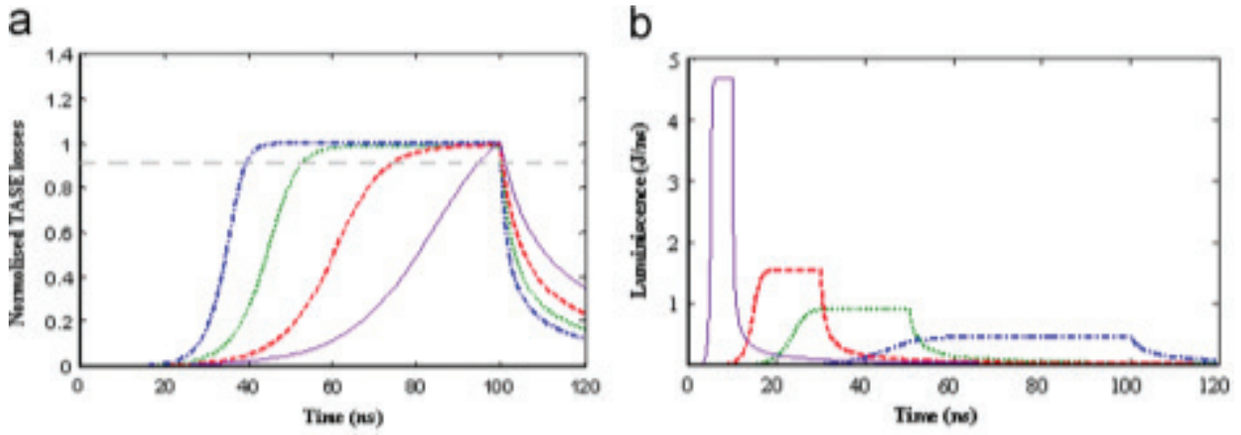


Figure 5. Fluorescence evolution of gain volumes vs. pumping time. (a) Normalized ASE to its maximal value for different crystal apertures, D: blue dash-doted curve D = 20 cm (E_{max} = 824 J, E_{loss} = 590 J), green dots D = 15 cm (E_{max} = 460 J, E_{loss} = 290 J), red dashes D = 10 cm (E_{max} = 210 J, E_{loss} = 100 J), and violet solid D = 6 cm (E_{max} = 74 J, E_{loss} = 20 J); (b) TASE for different pump pulse durations, τ_{pump} (15 cm crystal diameter): violet solid curve τ_{pump} = 10 ns (E_{loss} = 325 J), red dashes τ_{pump} = 30 ns (E_{loss} = 321 J), green dots τ_{pump} = 50 ns (E_{loss} = 315 J), blue dash-dots τ_{pump} = 100 ns (E_{loss} = 290 J).

durations are shown for 15 cm crystal diameter (**Figure 5b**). As seen, the losses slightly grow due to the higher pump rate that enhances TASE with reduction of the pump pulse duration.

If the total compensation of transverse gain by the index-matched absorber coating is not possible, the reflectivity from the side wall will be enough for parasitic generation-TPG. Therefore, one can establish the TPG threshold as an equality transverse gain of the crystal to absorption coefficient of its side wall. There are two most probable transverse modes which can develop: first one is due to the maximal population inversion which is a generation near two working parallel surfaces [23] and the z-pass between these surfaces due to total internal reflection [26] (**Figure 6a**). The latter mode surpasses the first one in large aperture crystals with a high aspect ratio and respectively low crystal doping because higher gain for second mode. One can define the TPG threshold small signal gain G_t through the pump intensity F_p as:

$$G_t = \exp\left(\frac{6}{zh\nu_p} \mathrm{D}\, F_p\right) \tag{1}$$

Introducing $K = D \bullet F_p$ as a K-parameter, we can find the dependence of pump fluence TPG threshold on the crystal diameter (**Figure 6b**) calculating K for different crystal geometry and used absorber.

$$K_s = \frac{\nu_p}{\nu_{em}} * ln\, G_t * \frac{z\, F_s}{lnB}; \quad K_z = \frac{\nu_p}{\nu_{em}} * ln\, G_t * \frac{z\, F_s}{2n} \tag{2}$$

There (2) are two formula of the K-factor calculations for two transverse parasitic modes consequently, the generation near working surfaces (K_s) and the z-pass between them (K_z), where D is the pump area diameter, G_t is the highest transverse gain that would be compensated by an index-matched absorptive coating, z is the crystal thickness, n is the index of refraction of the crystal, and the absorption coefficient for the pump frequency—B.

A crystal with a given aperture fixes the maximum pump fluence because the product of crystal diameter and the pump fluence is constant for each value of the critical transverse gain

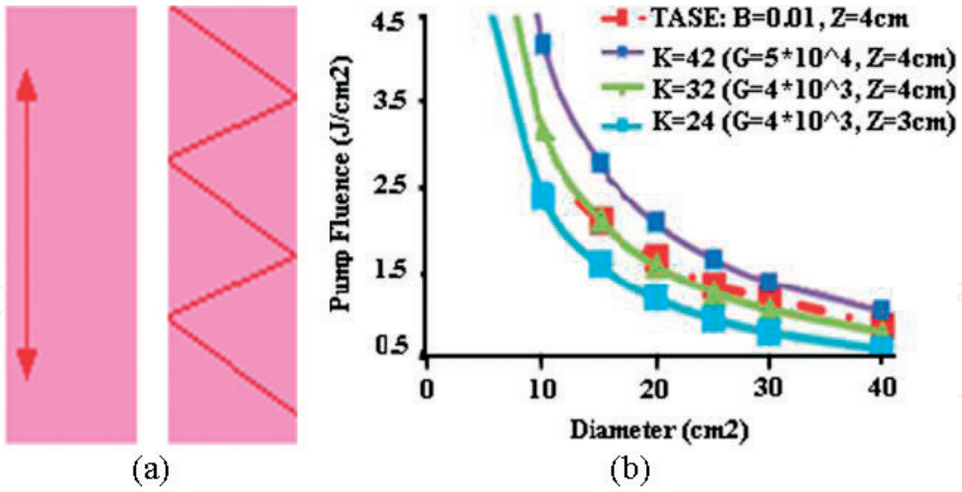


Figure 6. (a) Two transverse optical paths with highest gain for TASE within a crystal; (b) dependence of pump fluence on crystal diameter: solid curves: calculated for TPG (K = 24, light blue squares; K = 32, green triangles; K = 42, blue squares); dot-dashed curves: calculated for TASE (red squares: B = 0.01).

or index matching of the absorber and crystal thickness. Therefore, enlargement of the crystal aperture requires reducing the pump fluence. Moreover, the pump fluence will be limited for any crystals and absorbers because the complete matching is impossible for both polarizations of the transverse modes. The dependence of the maximal possible pump fluence on the crystal diameter was shown in **Figure 6b**, where the purple rhombus-marked curve is the ideal case of upper bound for 3 cm crystal thickness and reflectivity of σ-polarization under the condition of total index matching for π-polarization.

The same dependences can be built for TASE limitation based on the APs (**Figure 5a**, crosses with gray dashed line indicating 0.9 of the maximum volume). TASE curve for crystals with B = 0.01 nearly match the TGP curve with K values of 32 (these values correspond to existing absorbers [16]) and is located below the purple ideal curve as shown in the **Figure 6**. The main conclusion to be drawn from this correspondence is that there remains no motivation to develop better absorber materials, owing to restrictions of TASE. Therefore, the situation for laser amplifiers with large apertures appears bleak, especially with respect to their application as final amplifiers in very high power laser systems. For example, one can conclude from **Figure 6**, that for 20 cm crystal diameter, the maximum F_p is 1.5 J/cm² meaning the extracted fluence is about 0.7 J/cm², when saturated one for Ti:Sa crystal is 0.9 J/cm², which indicates the deeply inefficient amplifier operation. Nevertheless, below, we will demonstrate that the parasitic losses due to both TASE and TPG can be significantly reduced using EDP technique.

We suggest to change the conventional method of pumping and amplifying the multipass amplifiers to overcome the restrictions discussed above. Conventional method is based on the energy stored in the amplifier media prior to the arrival of the first pass of the input pulse [26]. We are able to forestall TASE and parasitic lasing and increase the extracted energy by continuing to pump after the arrival of the amplified pulse. In this case, the energy extracted during one pass of the amplified pulse through the crystal could be restored by pumping up to AP or TPG threshold before the next pass. An extended pump pulse duration ranging from tens to hundreds of nanoseconds, or several delayed pulses is required for EDP process. One

can get sufficient time in this case for proper pumping between passes, allowing increased total pump fluence due to the longer pump pulse duration and overcoming problems with temporal jitter. This approach was shown to double the output flux above the parasitic lasing limit in the experiments in University of Michigan [27].

Optimization of EDP method for presently available large aperture Ti:Sa amplifiers was made in Ref. [28] . The description of amplified transmission of pulses through the multipass amplifiers can be done by broadly applying Frantz-Nodvik solution for the 1-D photon transport Eq. [26]. Solution for optimal EDP-amplifiers can be rewritten as a single equation, in contrast to conventional amplifiers, where this equation is applied iteratively with adjustment of small signal gain for each pass, because the restoration of the population inversion by the pump between passes in case of EDP, and hence of the small signal gain, for each pass:

$$F_{out} = F_s \ln\left\{1 + \left[exp\left(\frac{F_{in}}{F_s}\right) - 1\right] exp\left(N \frac{\nu_{em}}{\nu_p} \frac{F_p}{F_s}\right)\right\} \tag{3}$$

where N is the number of passes, ν_{em} is the emission frequency, ν_p is the pump frequency, F_{out} is the N-pass output fluence, F_s is the saturation fluence, F_{in} is the incident fluence, and F_p is the initial pump fluence (before signal arrives).

Therefore, we simply introduce a factor of N into the small signal gain expression to get the output flux after N-passes of amplification. This could be easily proved by introducing the output flux from any $N-1$ passes as F_{in} for N-th pass and following the usual iterative procedure.

Dependences of the output fluence calculations for 4-pass amplification with conventional amplification and EDP for various pump fluence are presented in **Figure 7a**. From this graph, one can get the next conclusions. First—EDP amplifiers can deliver significantly more energy (up to four times for four-pass amplifier) compared to regular ones with the same initial pump fluence. Second—the input fluence that saturates the amplifier is much higher than that for the regular case because the graphs asymptotically approach to the value of four times of the initial pump flux multiplied by coefficient of quantum defect. From comparison of the two green or two blue curves in **Figure 7a**, one can see that the curvature slope becomes twice lower at 50–70 mJ/cm^2 of the input fluence for conventional amplifier and near 200 mJ/cm^2 for EDP-amplifier. We have a higher extracted energy with growing input flux and so are able to add more pump fluence between passes. So, the input fluence for amplification with EDP has to be much higher to make them efficient and the process of amplification mimics the case of a high value of F_s. On the other hand, this says us about a much higher energy capacity of the amplifier.

The optimal diameter for the pump area of the EDP-amplifiers can be demonstrated if into Eq. (3), in place of F_{in} and F_p, will be introducing the ratios E_{in}/A and K/D (2), respectively, where E_{in} is the total incident energy and A is the pump area. The dependences of the output energy on diameter of the pump area, for different K values and incident energies, are presented in **Figure 7b**. The output fluence of damage threshold was marked by the red dashed line. Using these graphs, we can calculate the highest output energy for amplification with EDP for a practically available liquid absorber and a crystal with 20–25 cm diameter [29].

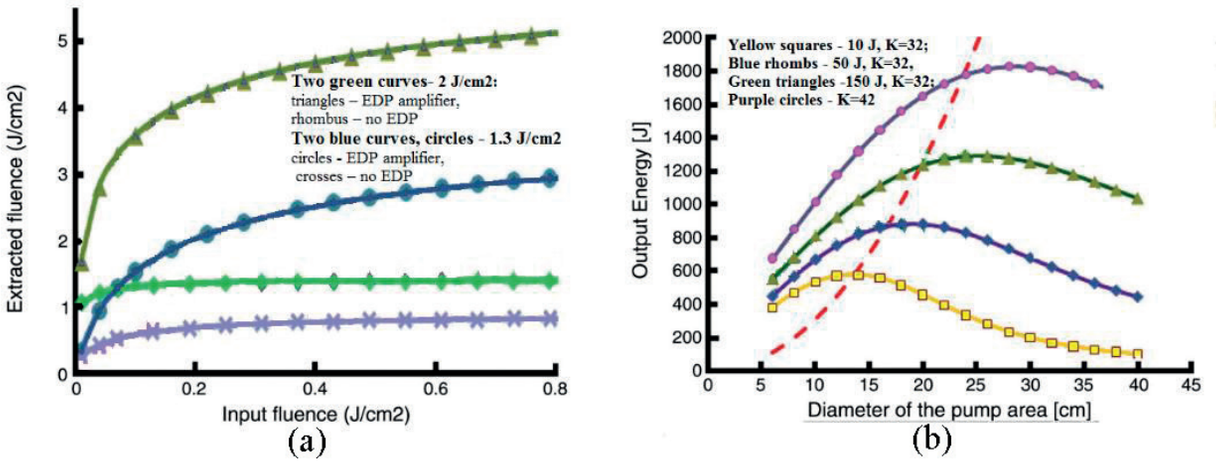


Figure 7. (a) Dependence of the output fluence of the 4-pass amplifier on the input fluence for several pump ones; (b) dependence of the output energy on diameter of pumped area for different input energies and K-factor; dashed red curve: damage threshold fluence.

This absorber is able to accommodate the maximum transverse gain of 4000, which leads to a value of $K = 32$. We can find the output energy of ~800 J from the blue rhombus curve in **Figure 7b**, which corresponds to 50 J input energy. In Ref. [16], the authors demonstrate the final EDP-amplifier 60 J, making 800 J realistic output energy for the next stage of amplification. This output energy can be reasonable for crystals with this diameter due to output fluence 2 J/cm^2 and the extraction efficiency close to theoretical one 65% which is reachable for EDP-amplifiers.

The EDP-technology was successfully spread out in the many world class laboratory for application in the ultra-high power laser systems, demonstrated today's world record near 200 J extracted energy and 5.0 PW output power [30]. Below several examples will be exhibited.

First time, this method was used in the 4-pass amplifier of the HERCULES-300 TW Laser [31]. Four-pass amplifier crystal was cooled cryogenically to 120 K avoiding wave-front thermodistortion of the output beam. Because the amplifier crystal was located in the vacuum chamber to avoid the surface deposition, cladding of the side surface was impossible. Extracted flux was increased from 0.6 to 1.2 J/cm^2 due to application of EDP [27].

The authors of [16] have successfully developed a high-energy Ti:Sa laser system that delivers 33 J before compression at 0.1 Hz using LASERIX-4-pass EDP-amplifier. 100 mm diameter Ti:Sa crystal (pumped area-60 mm) was used as the final amplifier which was pumped with 72 J of energy delivered by frequency-doubled high-repetition rate Nd:Glass lasers. The good amplification efficiency of 45% with a homogeneous flat-top spatial amplified intensity profile was finally obtained.

The EDP-method has also been applied on several Ti:Sa booster amplifiers of petawatt scale. One of them was 3-pass EDP-amplifier of APRI 1.5 PW CPA-laser (South Korea) [32]. The team of laser developers reported about the generation of 1.5 PW by using two stage final EDP-amplification with the maximum output energy of 60.2 J at a pump energy of 120 J.

Shanghai Institute of Optics and Fine Mechanics, Chinese 5 PW CPA: laser, 4-pass EDP-amplifier [30]. Effective suppression of the parasitic lasing in the final booster amplifier was done using the EDP-technology combined with index-matching cladding technique and the precise control of the time delay between the input seed pulse of 35 J and pump pulses of 312 J. The output energy of 192.3 J from the final amplifier was corresponding to a pump conversion efficiency of 62% to the output laser energy.

The design of the final EDP-amplifiers was recently developed for three pillars of the Extreme Light Infrastructure (ELI) project [33]. ELI is the ambitious pan-European laser research project. The major mission of the ELI facility is to make a wide range of cutting-edge ultrafast light sources available to the international scientific community. The first purpose of the facilities is to design, develop and build ultra-high-power lasers with focusable intensities and average powers reaching far beyond the existing laser systems. The secondary purpose is to contribute to the scientific and technological development toward generating 200 PW pulses, being the ultimate goal of the ELI project. PW-class lasers have been planned to build in the three pillars of ELI. 2 PW peak power, 10 Hz repetition rates and <20 fs pulse duration lasers will be part of the ELI-BEAMLINES and the ELI-ALPS, while the L4 of the ELI-BEAMLINES as well as the ELI-NP lasers aiming at 300 J/10 PW lasers. The roadmap for 200 PW laser facility was paved by the ELI consortium. This will increase the available laser power by at least one order of magnitude in its first three pillars, and on another more order of magnitude in its fourth ultra-high-intensity pillar. The laser power frontier was planned to be pushed into sub-exawatt regime by the establishment of ELI s fourth pillar.

The examples of final EDP-amplifiers design of 10s PW laser system are presented on the **Figures 8** and **9**. As the estimations demonstrate, the EDP-technology is able to significantly increase the output energy and intensity. There are calculated as optimal output parameters: the diameter of the pump area and crystal −19 and 20 cm, the pump energy −960 J, the input and the output energy −60 and 600 J. The losses with the EDP technology can be made under 5% (**Figure 8**).

The total losses in 4 cm thickness crystal of conventional amplifier is about 70%, and for 3 cm, it is −80% as seen from the **Figure 8a**, and significant gross begins from 30 and 20 ns of the pump, respectively. On the **Figure 8b**, dependences of losses for optimal extraction of the 3-pass and 4-pass EDP amplifier are demonstrated with the crystal thickness of 4 cm.

For 3-pass, the delay between passes 1 and 2 is about 20 ns and 2 and 3–30 ns, whereas the scheme with delays between passes of the 4-pass amplifier (15, 20, 30 ns) is presented also in the **Figure 8**b. Taking in account the compressor transmission efficiency 70% [32], the compressed energy up to 400 J can be expected. Output peak power about 30 PW can be reached in one channel with pulse duration 10–15 fs. This amplifier could serve as a building block for ELI fourth pillar, and seven EDPCPA channels will be enough for approaching 200 PW.

As a final remark of this part, we can emphasize that there is a big gap between the reached now output energy of 200 J and potential possibilities of the EDP amplifiers of 600–800 J extracted energy with today's available Ti:Sa crystals, which should be filled in the closest future. Moreover, manufacturers are working now under the larger aperture Ti:Sa crystal and

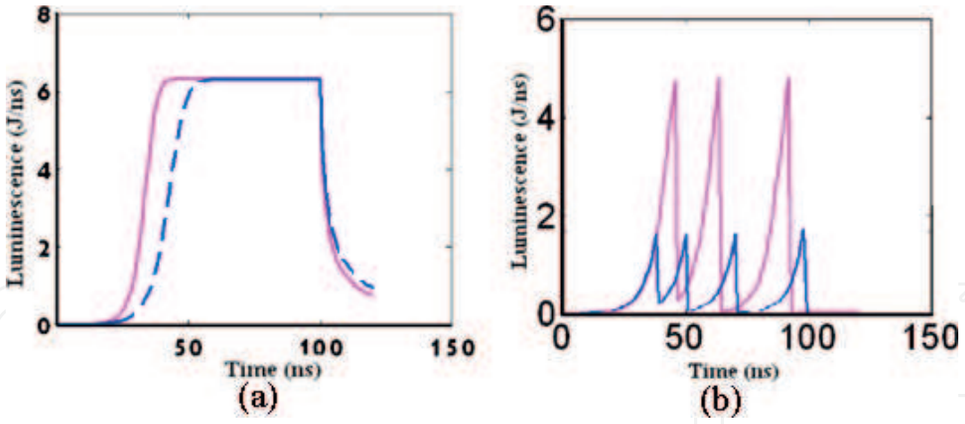


Figure 8. Dependences of losses for 4 (blue-dashed curve) and 3 cm (pink-solid curve) thickness of the crystal: (a) conventional amplifier; (b) EDP-amplifier.

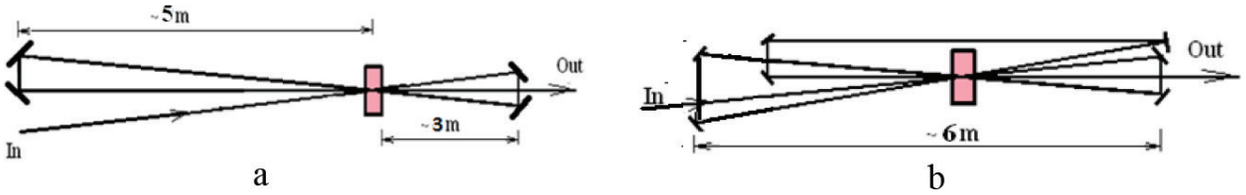


Figure 9. Final EDP-amplifiers with 3- and 4-passes: (a) EDP amplifier with a 19-cm-diameter pump area can approach 500-J energy with a 60-J input (100 J losses) during 3-pass; (b) 4-pass EDP amplifier with a 19-cm-diameter pump area can approach 600-J energy with a 60-J input, when pumped by 960 kJ (28 J losses).

have reached 30 cm crystal diameter. The estimations demonstrate the 40-cm crystals with 6-cm thickness which is nearly maximum for EDP amplification due to geometric reasons. This amplifier is able to supply ~3 kJ/140 PW with 250 J of seed energy while suffering TASE losses of about 207 J. Two EDPCPA channels will be enough for approaching 200 PW in this case.

3. Pulse duration shortening

3.1. Preserving and restoring pulse spectral bandwidth

Here, we will concern another way of the peak power increasing, namely pulse shortening. It was discussed above that the gain narrowing and saturation limit the achievable pulse duration to about 30 fs [30, 31]. To achieve the 10–15 fs pulse duration designed for the Apollon system as well as for the 10 PW laser of the ELI [18], further scientific and technological efforts have to be made to avoid spectral narrowing in the power amplifiers.

The idea to use optical rotatory dispersion (ORD) (the angle of polarization rotation dependence on wavelength) spectral filter was suggested for conservation of bandwidth in low gain multipass Ti:Sa amplifiers, typically used for the intermediate and duty end amplifiers of multi-TW-PW class systems [34]. The spectral gain can be effectively re-shaped using difference of

π- and σ-emission cross-sections of Ti:Sa crystal which will result in the keeping bandwidth of efficient amplification [13]. The overall amplification process can be kept lossless and efficient as the effective spectral gain is tuned, unlike to the spectral shaping of the pulse. This technique is especially advantageous for amplifiers where the energy extraction is of major importance in intermediate and duty end ones of ultrashort pulse large-scale laser systems.

The optical rotatory dispersion (ORD) is applied to encode/decode the polarization state of the amplified spectrum in addition to using both π- and σ-emission cross-sections. Polarization vectors of spectral components are encoded before amplification using an ORD quartz crystal (right rotating quartz in **Figure 10b**) with a resulting distribution between π- and σ-cross-sections (**Figure 10a**).

The emission cross-section of σ-polarized light is nearly 0.4 of the π-polarized light. The sides of the spectral band are aligned toward the π-axis, while the components around the central and most intense part of the spectrum are directed closer to the σ-axis. This allows shaping of the spectral gain so the gain narrowing can be substantially reduced or eliminated at all. The second quartz crystal (left rotating quartz in **Figure 10b**), with an opposite sign of ORD decodes the polarization state of spectral components after amplification. The whole polarization encoded spectral distribution fits between π- and σ-directions by using of two achromatic λ/2 plates. A temporal walk-off between the π- and σ-components due to birefringence in Ti:Sa can be compensated by the addition of an undoped, but orthogonally oriented sapphire of the same thickness.

The 10 Hz, mJ laser system of the Max Born Institute was using proof-of-principle experiment (**Figure 11**). The 20 fs pulses from oscillator were stretched to 120 ps and amplified in a 10-pass Ti:Sa amplifier to ~1 mJ. The pulses with 35 nm bandwidth were compressed using a diffraction grating compressor to their transform limited pulse duration of 28 fs.

The computer modeling of the PE-CPA amplifier resulting in the broadest bandwidth showed an optimum thickness of 17.5 mm of the quartz crystal (**Figure 10b**). A spectrally dependent model of amplification of strongly chirped pulses was used for modeling the PE-CPA amplification. It includes ORD encoding, saturation of amplification and decoding of polarization vectors. The polarization encoded amplifier was built in a 6-pass configuration with a Ti:Sa crystal of 15 mm thickness (**Figure 11**). It was pumped from both sides by the second harmonic beam of a Q-Switched Nd:YAG laser. The pump diameter was de-magnified from 6 mm to 2.5 mm by two lenses (focal lengths 1 m) to fit it with the diameter of the seed pulse. An undoped sapphire

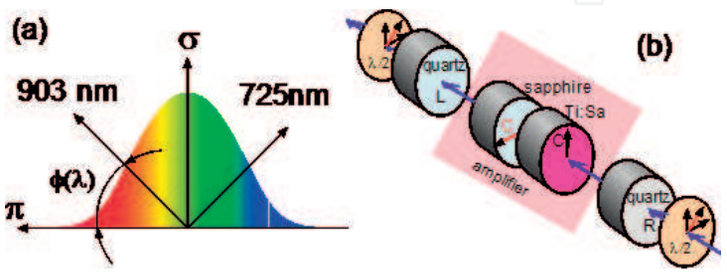


Figure 10. Distribution of polarization directions of spectral components by a 17.4 nm ORD quartz (a); principle schematic of the polarization encoded amplifier (b).

was mounted next to the Ti:Sa crystal (both with thickness of 15 mm). Both crystals had orthogonally directed C-axis to compensate for the inherent temporal walk-off. The incident angles of amplified beams on the active medium were kept as small as possible to minimize uncompensated walk-off and the total length of the amplifier was set to 2.1 m. To eliminate the spectral interference fringes from the outgoing amplified spectrum, the sapphire crystal was mounted on a fine rotator stage and was adjusted. The compressed pulses were loosely focused into a 5 mm BK7 glass plate by a lens (focal length 3 m) with the most homogeneous part of the SPM signal filtered out by a pinhole located at the focus of the lens. Using this technique, the bandwidth of the seed pulse was broadened in self-phase modulation (SPM) stage and stretched in the bulk (**Figure 11**) to show the broadband amplification capability of the scheme.

A multi-passing SF6 glass block (80 cm path) was used for stretching the broadband pulse with a near top-hat spectral profile and a bandwidth of 91 nm, the last one was then collimated by a lens (focal length 1.5 m). The seed pulse energy was about 35 μJ due to the energy losses at the pinhole, as well as two metallic mirrors used in the bulk material stretcher and reflections on surfaces of the uncoated ORD quartz.

The polarization encoded amplification was tested for a high (~200) and low (~30) gain case to demonstrate the effectiveness of the PE-CPA method. The broadband seed was initially amplified without polarization encoding in order to form a baseline (**Figure 12a**) with a gain of about 200. The gain-narrowed feature with a resulting bandwidth of less than the half of the seed was demonstrated at the recorded spectrum. The output spectra closed to the input seed resulted in FWHM bandwidth of 82 nm using polarization encoded amplification. A dip was produced at the center due to the spectral edges of the spectrum that experienced a high gain. The following experiments demonstrated that spectral-dependent gain feature can even broaden the bandwidth depending on the initial shape of the seed spectrum and an amplifier saturation.

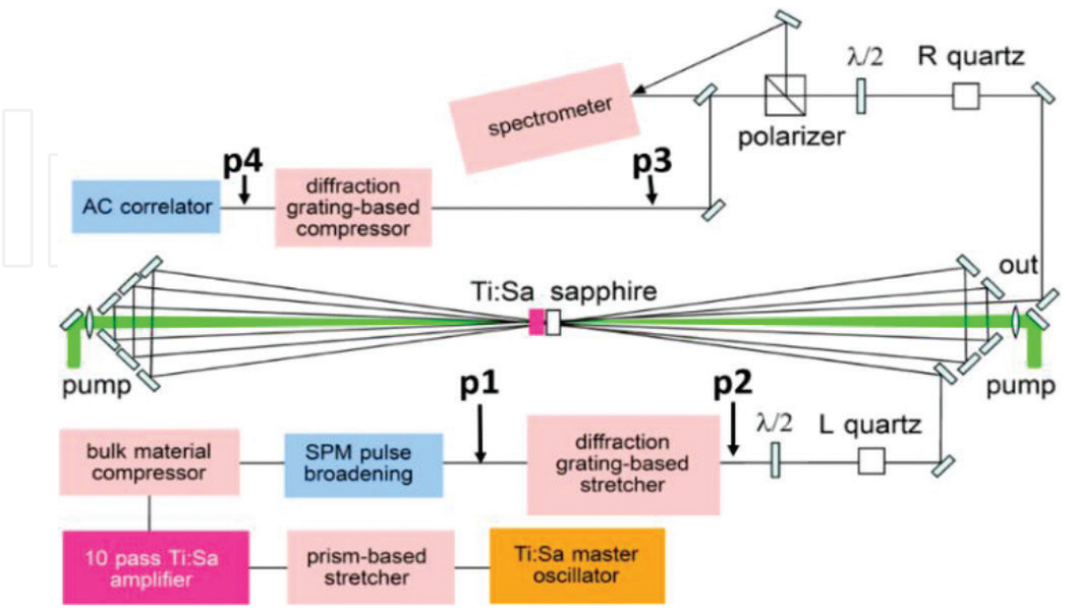


Figure 11. Schematic of the experiment system. Spectra were measured at places p1–p4.

Seed pulses (energy ~200 μJ) were sent directly to the amplifier, by-passing the compressor and SPM stages to investigate the low gain scenario. A pulse with a bandwidth of about 48 nm was achieved after polarization encoded amplification with a net gain of ~30. In contrast to the top-hat seed spectrum (**Figure 12a**), the amplified Gaussian spectrum is almost 40% broader compared to the seed due to the high-gain experienced by the spectral wings (**Figure 12b**).

It was also shown that an additional polarization rotation takes place during the pulse amplification, substantially changing the conditions of high-energy amplification and introducing the distortion into initial polarization encoding. Despite the additional polarization rotation occurring during amplification impeding the decoding process, the energy efficiency of the back conversion to the linear polarized state can be improved by increasing the thickness of the second quartz crystal. The computer modeling shows that an efficiency as high as 99% to convert energy to a linear polarized state for moderate gain values can be reached with the optimal thickness of the second quartz.

Good compressibility of spectrally shaped PE amplified pulses is highly important for the practical application of the PE-CPA method. For testing its compressibility, the pulse spectrum was broadened to ~72 nm during the PE amplification and then compressed down to compressor consisting of two diffraction gratings. The compressor reduced the bandwidth to ~ 60 nm. Single-shot second-order autocorrelator (AC) was used for pulse duration measurements. The width of the measured AC trace is 28.0 fs which corresponds to the pulse duration close to 18.5 fs.

The computer modeling shows that a 200 nm spectrum is achievable at a multi-joule level in a PE-CPA Ti:Sa amplifier with seed pulses broader than the experimental bandwidth. This output requires seed pulses with a smooth spectrum preferably with a Gaussian shape. The computer modeling of the output spectras of 4-pass PE-CPA amplifier seeded by a 2 J Gaussian-shaped pulse (FWHM of 180 nm) and pumped by 50 J is shown in **Figure 13**. The spectrum is broadened to 200 nm after amplification. Nearly, 30% depolarization losses (**Figure 13a**) can be compensated by doubling the thickness of the decoding quartz (**Figure 13b**).

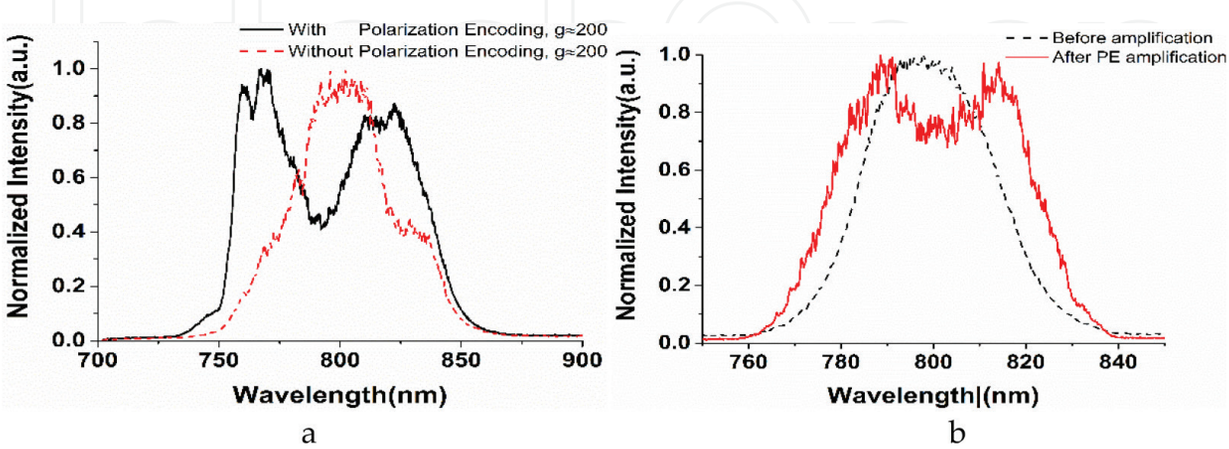


Figure 12. (a) Amplified spectra with (solid line) and without (dash line) the PE technique under a high gain amplification; (b) spectra before (dash line) and after the PE amplifier (solid line) at a gain of 30.

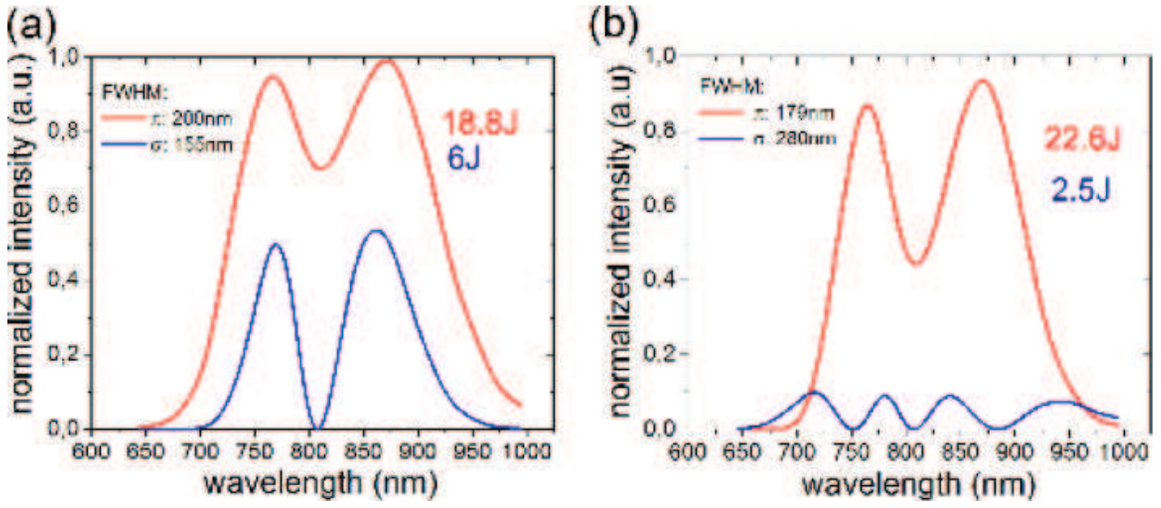


Figure 13. PE-CPA amplifier (simulation): (a) thicknesses of encoding and decoding quartz plates are equal (17.4 mm); and (b) the second quartz plate is 35 mm thick. The seed pulse has a Gaussian spectrum with FWHN = 180 nm. Pump energy: 50 J, seed energy: 2 J, 4 passes.

High-energy polarization encoded Ti:Sa amplifiers are able to deliver an amplified bandwidth of 200 nm, which was predicted by detailed modeling, making it a promising technique for intermediate and final amplifiers of high field Ti:Sa CPA-laser systems. This technique may pave the way to PW class Ti:Sa lasers with tens of Joule few cycle laser pulses.

3.2. Multiple compression stages

The multiple compression method based on spectral broadening using self-phase modulation (SPM) in the bulk of material with the further recompression of the chirped pulse is able to deliver even shorter pulse duration (potentially below 10 fs) without energy sacrificing. Previous attempts were not suited for the highest powers because it used SPM with combination of spatial filtering in near field [35, 36] in order to provide spatially uniform phase due to the axial uniform part of the Gaussian distributed intensity. These approaches were restricted to only mJ-level of the output energy.

In Ref. [37], the next logical step was suggested to use super-Gaussian beam profile due to its higher uniformity. If a laser beam has spatially uniform intensity, SPM can be used in near-field without spatial filtering and consequently eliminating constraints of the laser energy and transmission efficiency. In a proof-of-principal experiment, spectral broadening of 30 nm pulse spectra to ~80 nm was demonstrated. A flat-top beam profile of the HERCULES laser [31] at 30TW power level was used for SPM spectral broadening and compression of a fraction of this power from 30 to 14 fs by a prism-based compressor was fulfilled. The laser pulse with the energy about 1 J and 6 cm beam diameter was directed at intensity ~1 TW/cm^2 on the bulk of fused silica plate after compression by the standard grating compressor to 30 fs. Glass plates of 0.8, 2 and 2.5 cm thicknesses were used for SFM in the experiments. After that, the 100 times attenuated energy and reduced to 1 cm diameter beam was directed into the prism compressor. The spatially resolved spectrum of the pulse was measured and shows the deviation of the energy within 6% through most part of the beam aperture. It follows from **Figure 14a** that the

initial FWHM of the space-integrated spectrum ~30 nm was broadened to ~80 nm with the 2 cm glass plate.

The final compressor consisted of two prisms (glass SF10) separated by ~50 cm, after which the single-shot autocorrelator was used for pulse duration measurement. **Figure 14b** and **c** demonstrate the autocorrelation picture and trace lineout, respectively. The initial nearly-transform limited pulse, with the duration from the FWHM autocorrelation trace of ~30 fs was shown on **Figure 14b** and the solid blue curve in plot (c) inferred assuming Gaussian pulse-shape. The pulse after the SPM used with the 2.5 cm glass plate and recompression is shown by autocorrelation (b) and the dashed pink curve in plot (c). The compressed pulse duration exhibits shortening by a factor of 2 leading to ~14 ±1 fs.

During these experiments, the instability from shot to shot of the output pulse shape, distribution of the significant part of the energy into wings (**Figure 14b** and **c**) and high level of the white light generation were observed. The distortion of the output pulse shape and its instability is a result of uncompensated third-order dispersion (TOD) of prism compressor that was used as second stage of compression. Besides, TOD coefficient in nonlinear Schrödinger equation of laser pulse propagation through transparent media is inversely proportional to the third power of the pulse duration and the pulse duration consequently varies inversely with incident peak intensity due to SPM. This is why even small fluctuation of the incident intensity leads to significant distortion of the shape of the compressed pulse. A solution of these two complications could be the replacement of the prism compressor with chirped mirrors with compensated TOD. Using about 10 bounces on the chirped mirrors and the glass plate at Brewster angle promises compressor throughput above 90%.

On the other hand, reducing the white light generation could also be possible since the main processes involved in this generation are efficient only when phase matching conditions are fulfilled, which could be destroyed by correctly choosing incident intensity and glass plate thickness. Evidence of such possibility can be found in Ref. [36], where the SPM was done

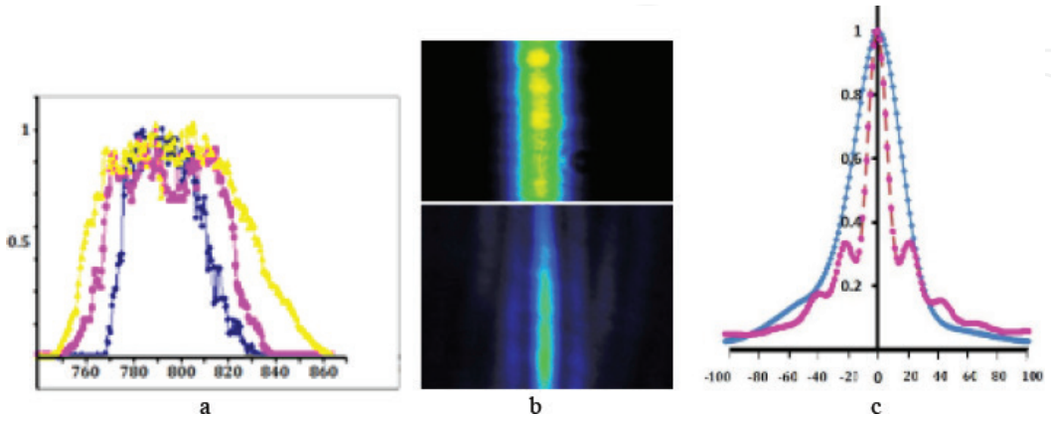


Figure 14. (a) Pulse spectrums: yellow curve (triangles): SPM with glass plate of 2 cm thickness, pink curve (squares): with plate of the 0.8 cm and blue curve (diamonds) represent the spectrum without the glass plate (no SPM); (b) autocorrelation of compressed pulse after SPM, (c) autocorrelation trace of the initial transform limited pulse (solid blue line) and compressed pulse after SPM (dashed pink line).

with a 3 mm glass plate and incident intensity of 8 TW/cm^2, and resulted in a very low level of the white light generation.

Further development of this idea was done in Ref. [38], where SPM in thin film (within 1 mm) and much higher intensity (up to tens of TW/cm^2) was suggested. This technique is able to significantly reduce the instability and white light generation discussed above and is capable to compress 25 fs large energy pulses as high as 1 kJ to the 1–2 fs level. In order to demonstrate the potential of thin-film-compressor, numerical simulation was done with the following initial beam parameters: central wave length 800 nm, pulse duration T = 27 fs, flattop transverse intensity distribution with diameter 160 mm and total energy 27 Joules. Thicknesses of the first and second thin film elements for SPM are 0.5 mm and 0.1 mm. The fundamental peak intensity is 4.7 TW/cm^2, after the first and second stages with temporal recompression procedure 16.6 TW/cm^2 and 43 TW/cm^2 at pulse durations 6.4 fs and 2.1 fs correspondingly.

As a conclusion of this part of chapter one can deduce, the discussed technologies of the pulse shortening are able to reduce the pulse duration to additional one order without energy sacrificing, which means the output peak power of a few hundred PW are possible from the single channel of CPA laser systems.

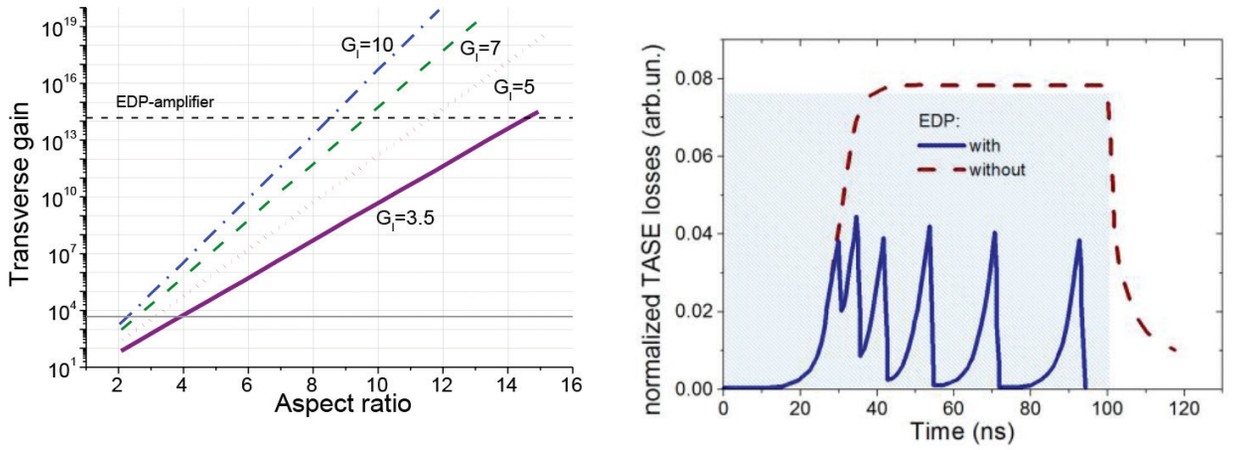
4. High repetition rate of ultra-high peak power laser systems

As it was discussed in Introduction (Section 1.3), the applications of the ultra-high peak power laser pulses required also high repetition rate or the other words high average power laser systems. Limitation of the high peak power laser systems on the repetition rate can be overcome by TD-technology and hence can increase their average power. Making the active medium thin reduces the longitudinal gain, which can be compensated by increasing the concentration of active ions and/or using crystals with higher emission cross-section, and the most promising crystal with required characteristics for these amplifiers is Ti:Sa. However, the attempt to increase the longitudinal gain leads to a dramatic growth of the gain in the transverse direction of the active medium. Therefore, TASE and TPG are strongly dependent on the axial gain and the ratio of the pumped area diameter to the crystal thickness (aspect ratio). For thin Ti:Sa active media, these effects cause significant depletion of the inverted population, and hence limit the extracted energy, the same way as it was detailed discussed in Section 2.

The EDP-technique was suggested to be applied for TD crystals [39] and successfully tested [41] mostly in powerful final stages of ultra-high peak power laser systems with hundreds of TWs to tens of PWs power, which are operating in the saturation regime. The overall gain of the amplifier can be kept as small as ~10–20, since the extraction of energy is a major importance. On the other hand, a large amplifier aperture is required for the high energy level. Therefore, power stages of the said Ti:Sa systems require a crystal size ranging from 5 to 20 cm, contrary to "conventional" TD amplifiers with the aperture of few millimeters where several tens of passes can be done [40]. The reasonable number of passes through the amplifier in this case, is restricted up to 6 due to geometrical complexity and available space. These two requirements form the lower boundary for the small signal gain of 3–5 per pass or the saturated one of 1.5–2.

Figure 15a demonstrates dependence of the transverse gain on the crystal aspect ratio for different longitudinal small signal gain values, which correspond consequently to the absorbed pump fluence F of $G_l = 10 – F = 3.8$ J/cm^2, $G_l = 7 – F = 3$ J/cm^2, $G_l = 5 – F = 2.5$ J/cm^2 and $G_l = 3.5 – F = 2$ J/cm^2. The maximal possible suppression of transverse gain using a conventional method of the side surface cladding and its combination with the EDP-method correspond two horizontal lines (solid and dashed line in the figure). The side surface cladding with a commonly used liquid absorber is considered in both cases. The conventional method of transverse gain compensation supports the aspect ratio between 2 and 4, as seen from this picture, while the EDP-amplifiers can afford 8–15. That means the latter one can be applied as TD-amplifier and can increase the output energy up to 16 times. The maximum value of aspect ratio can be determined from these calculations taking into account the required output energy and crystal thickness. Then, the small signal gain could be chosen depending on amount of pump passes and the crystal doping that will support the required absorption. For example, EDP is able to afford for the small signal gain of 3.5, the highest aspect ratio 15 with the reasonable amount of signal passes of 4–5. So, the Ti:Sa crystal of 15 cm is required for 10 PW laser (300 J); this corresponds to the crystal thickness of 1 cm and doping according to the chosen pump absorption.

As for conventional amplifiers, the EDP method can be applied in a similar way to thin disks amplifiers [28]. This method allows in optimum conditions to significantly reduce the losses in the crystals with the big aspect ratio, or in thin disk crystals (to 5–15%). The EDP method requires an extended pump-pulse duration ranging from tens to hundreds of nanoseconds, or a train consisting of several delayed shorter pulses. EDP can then be naturally combined with thin disk Ti:Sa amplifiers with regularly doping crystals because a smaller portion of the pump energy can be absorbed in smaller crystal thickness per pass. Choosing the correct distances of the pump and the seed pass shoulders, the multipassing pump can be adjusted for the optimum EDP. We demonstrate further that a new line of the CPA ultra-high intense high average power laser systems can be opened by combination of EDP and TDT with a possibility to be scaled up to tens of a PW peak power and hundred Hz-repetition rate.



a b

Figure 15. (a) Dependences of transverse gain on crystal aspect ratios; (b) losses calculated for the 200 TW/100 Hz 6-pass Ti:Sa EDP-power amplifier. Shaded area is the pump pulse.

As an example, losses have been calculated in a 20 × 2 mm Ti:Sa crystal pumped with 11 J (532 nm, 100 ns) and seeded by 180 mJ using the method elaborated in Ref. [25] with some modification of the computer model. According to these calculations, TASE loss without EDP (dashed curve in **Figure 15b**) is ~80%, the output energy for an EDP-amplifier is 6 J, while energy loss (solid curve) is ~10–15%. The peak power of the laser can reach 120–400TW if compressor transmission efficiency is 70% and pulse duration is 10–30 fs, while the average power is close to 0.6 kW at the repetition rate of 100 Hz.

Proof-of-principle experiment of the operation of a broadband EDP-TD amplifier in a 100 TW CPA laser system was presented in Ref. [41]. The amplifier head was fully characterized, including measurement and modeling of the temperature distribution, dynamics of amplification, and wave front of the amplified pulses.

Test bed was assembled in Max-Born-Institute on the base of commercial CPA laser system amplifier, which produces 100 TW peak power, 28 fs laser pulses at 10 Hz repetition rate. The final cryogenically cooled Ti:Sa amplifier has been replaced in experiments with the EDP-TD room temperature cooled arrangement (**Figure 16**). Ti:Sa crystal with a 35 mm diameter, 3 mm thickness and an absorption coefficient of 2 cm^{-1} was mounted in the home-made thin disk head module. The active mirror scheme was applied for the amplifier. Rear side of the crystal was HR coated, while the front one was AR coated, for both pump (532 nm) and seed (800 nm) wavelengths. The sides surface of the Ti:Sa crystal was coated by the absorbing material (refraction index of 1.76 at 800 nm), for TASE and TPG suppression. The rear surface of the crystal was actively water cooled to room temperature. Three temporally synchronized lasers, each providing 15 ns, 2 J pulses at 532 nm wavelength pumped area of 24 mm diameter.

Each of the three pump beams passed through the thin disk twice, one pass includes the reflection from the rear surface of the crystal. The total absorption for double pass of pump was measured to be 85%. The vertically separated pump beams one can see on the side view of the **Figure 16** with the smallest incidence angles, where the pump 2 was omitted. Three passes (mirrors S1-S5) amplified a positively stretched seed of few 100 ps pulse duration (energy −0.5 J) with a total gain of about 5.

Severe parasitic lasing was generated despite the use of the liquid absorber in the absence of the seed, when the active medium was simultaneously pumped with total absorbed energy 3.4 J by the double passed pump beams 1 and 3. This is clearly visible on the oscillogram of the luminescence (**Figure 17a**) from Ti:Sa crystal. EDP technique was applied to avoid TPG losses, extracting energy from the crystal before the second pass of the pump 3 (~3 J of absorbed energy). After first pass of the pump 3, the second one added 0.4 J to the stored energy delaying about 20 ns after the extraction of 0.5 J by the first seed pass (total amplified energy after the first pass was about 1 J). To avoid another round of parasitic generation, the pump pulse from the pump laser 2 was added between the second and third seed passes (**Figure 17b**), which allowed to reach 2.6 J of the amplified energy when the total absorbed pump was about 5 J. Three passes amplification only and two passes of the pump were required for this seed to achieve almost 50% extraction efficiency (compared with tens of passes of conventional Nd:YAG or Yb:YAG TD amplifiers) due to the much greater emission cross-section and

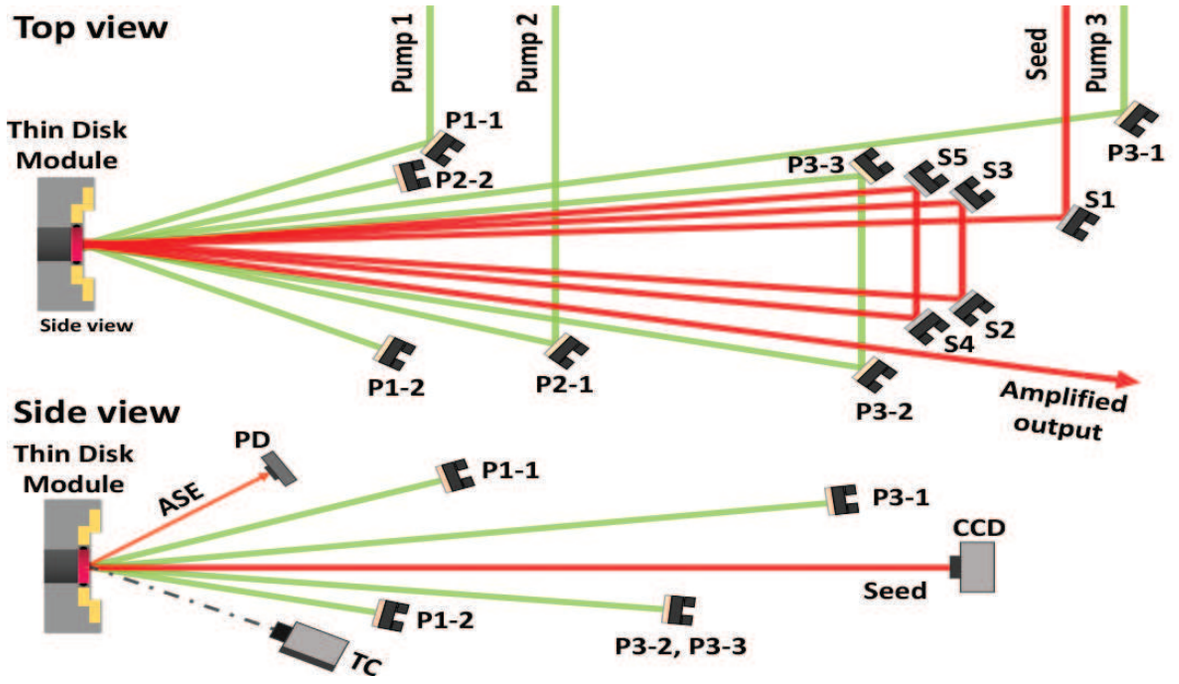


Figure 16. Experimental set up. The layout of the seed amplification consists of mirrors S1–S5 (red lines). The green beams are pump. Mirrors P1-1 and P1-2 were used for pump laser 1, mirrors P2-1 and P2-2 were used for pump 2, mirrors P3-1, P3-2 and P3-3 were used for pump 3.

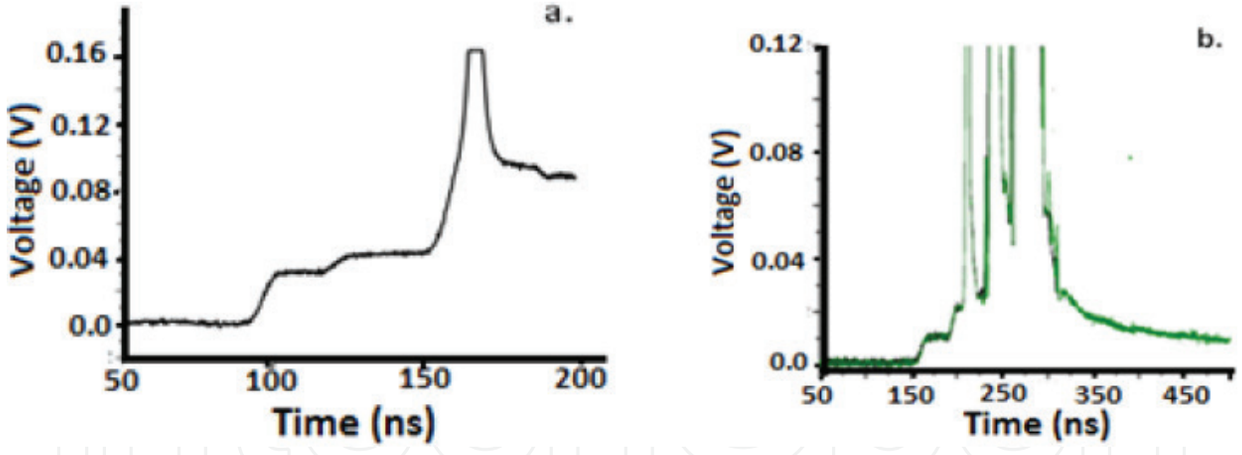


Figure 17. Oscillogram of the luminescence from Ti:Sa crystal. (a) Parasitic generation after double pass of the pump beams 1 and 3 with total absorbed energy about 3.4 J; (b) the luminescence with three seed passes.

thickness of the Ti:Sa crystal. The typical near field cross-section of pump and seed amplified after the third pass beams had the flat-top shape with the good uniformity.

The temperature distribution over the crystal input surface in the transverse direction through the crystal was measured (**Figure 18a**) with a thermal imager. The crystal was pumped with 4 J of pulse energy at 10 Hz repetition rate without the energy extraction by the seed. Average flow speed was about 7 cm^3/s with the initial temperature of the coolant 18°C.

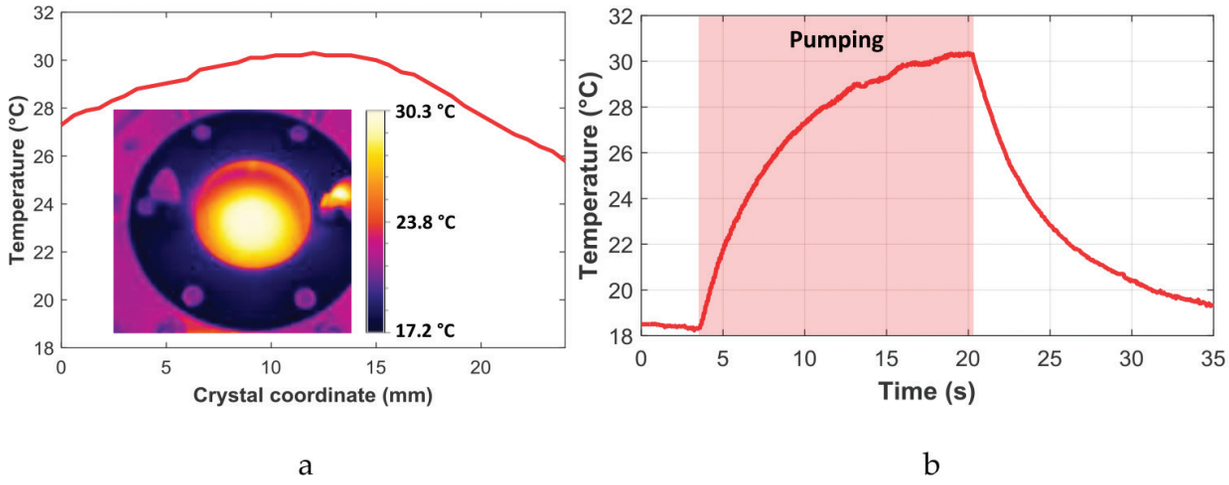


Figure 18. (a) Cross section of temperature distribution in the amplifier crystal after heating stabilization during pumping by the 4 J per pulse at 10 Hz repetition rate. The curve shows the temperature distribution of the horizontal mean section of the pumped area (red, solid line) and temperature distribution in the amplifier head (inset); (b) central point temperature growth dynamic of Ti:Sa crystal.

Figure 18b shows the temperature growth dynamic taken at the central point of the crystal until temperature stabilization. As seen from this curvature, the stabilization was reached after the crystal pumping within 20 s with 10 Hz repetition rate of the pump pulses. **Figure 18** shows that a coolant temperature of 18°C was sufficient to keep the maximal crystal temperature after stabilization under 30°C. The variation through the pump area was only 3°C, which does not significantly affect the seed beam wave front. The liquid absorber consumed a TASE absorption which is the largest portion of total luminescence; so, most of the pump energy was transmitted to the crystal heating. That means, similar result could be seen with the same crystal pumped with 8 J at the same repetition rate, when half of this energy is being extracted by the seed. Furthermore, a higher coolant flow speed could reduce significantly highest temperature.

The impact on the beam wave front was also measured during these crystal heating conditions. Measurements were taken until the crystal temperature was stabilized. The wave front before and after pumping was measured and consequently demonstrated P-V: 0.32 μm, RMS: 0.06 μm and after heating stabilization P-V: 1.51 μm RMS: 0.39 μm. These results are better than the comparable single-shot laser systems with side extraction of the heat measured before wave front correction [42].

Heat extraction from the Ti:Sa thin disk was numerically modeled to match experimental conditions and scale-up the system for higher repetition rates of 100 Hz, corresponding to 360 W of the thermal load. These model parameters account for the 8 J pumping with an energy extraction efficiency by amplification of the seed pulses of 50%. Proper cooling conditions were considered using a flow velocity of 5 m/s, and coolant temperature of 5°C. According to these simulations, the temperature profile is much more symmetric and smoother in the thinner crystal than in thick one. For 3 and 2 mm crystals, the temperature difference between the center and the edges was improved with central peak temperatures of 83.5 and 73.5°C, respectively.

The obtained results demonstrate the capacity to build a room temperature cooled final amplifier, providing few Joules energy of the seed laser pulses with in a 100 s TW/100 s Hz CPA laser systems.

Numerical modeling of scaling larger peak power amplifier modules with double channel cooling and double crystals (three cooling channels) design were also conducted in Ref. [43].

Double channel cooled disks with diameters ranging from 6 to 20 cm and corresponding thicknesses of 0.6 to 2 cm, were investigated (**Figure 19a**). The inlet flow velocity was 4 m/s in all cases to ensure high levels of heat extraction from the disk gain modules. Every gain module would remain under 45°C up to 40 Hz of operation relative to the coolant temperature. When the repetition rate is growing up further, one can see significant rise in the temperature increase (TI), nevertheless, the temperature profile would remain smooth and flat in the region of the laser amplification. Peak power could reach 8.5 PW and an average power 17 kW with compressor efficiency of 60% and pulse duration of 20 fs [**Figure 19a** (inset)]. The maximal repetition rate when amplifiers could operate safely and without serious beam degradation can be estimated based on the obtained TIs. Extremely efficient heat extraction can be obtained by increasing the diameter, while maintaining the aspect ratio of the gain disks with two coolant channels and thus flat temperature profiles with high repetition rate operation.

Further increase of the average power could be achieved by splitting the gain disk to multiple plates with reduced thickness and increasing the number of coolant channels. Four gain modules with double disk sizes ranging from 6 to 20 cm was investigated, with three coolant channel arrangement (**Figure 19b**). These simulations demonstrate 2 kW output average power with a TI in the disks of 21.5°C, and 28 kW average power at TI of 36°C using multiple disks and cooling surfaces with proper coolant flow conditions.

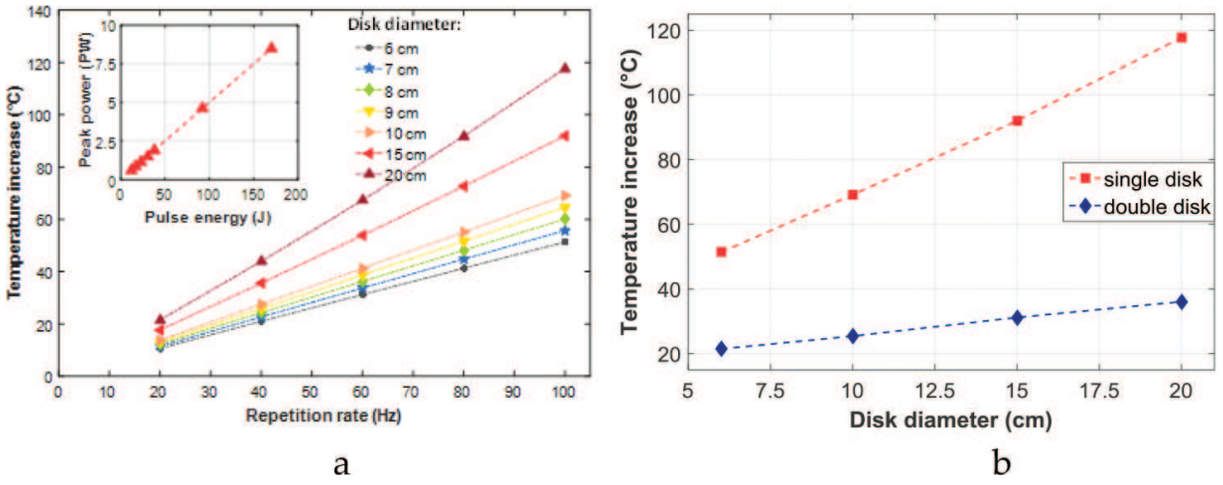


Figure 19. (a) Temperature dependence on repetition rates for various single disk sizes. Pump energy 40, 57, 77, 101, 127, 308, 567 J, for the diameters starting from 6 cm respectively. Peak power of compressed pulses listed in inset (compressor efficiency-60%, repetition rate-100 Hz and pulse duration-20 fs); (b) temperature in the single and double disk modules (Ti:Sa crystals of 6, 10, 15 and 20 cm diameters, 100 Hz for all cases) cooled by three channels using 4 m/s flow velocity at the inlet boundary of the channels.

Summarizing this investigation, we can conclude that the replacement of regular thickness Ti:Sa crystals in the booster/final amplifiers of ultra-high pack power laser systems on EDP-TD Ti:Sa amplifiers allows significantly to increase the repetition rates at an average power. These systems could reach such new frontier parameters as 100 s TW/100 s Hz and up to 1 kW output average power, using room temperature cooling systems and existing now pump lasers, which are able to deliver few Joules in green with the same repetition rate. At the same time, there are no limitations for further growing these parameters up to few PW peak power and 100 Hz repetition rate after developing the pump lasers required for that.

5. Conclusion

In this chapter, several ideas for innovation of the ultra-high peak power CPA laser systems were presented. Exploiting these ideas, one is able to significantly increase the output energy (up to KJ-level), reduce pulse duration (down to few fs) and so increase output peak power up to 100 s of PW. At the same time, the possibilities of average power growing of these systems up to 10 s kW was also demonstrated.

EDP-method for Ti:Sa final amplifiers was revealed as easiest way to reach a very high output energy [25, 27, 28]. EDP amplifier, when operated under the optimal conditions, is capable of significantly increasing the extracted energy and reducing the losses connected with TASE and TPG. With the existing large aperture of Ti:Sa crystals and index-matched liquid absorbers, it is possible to approach the sub-kJ level of extracting energy. With 70% compressor transmission efficiency and 15 fs pulse duration, about 30 PW power level could be reached. The powerfulness of EDPCPA technology was proved by spreading the method in the many world class laboratories and reaching recently the output energy about 200 J and world record peak power of 5 PW. Next steps of the output energy ~ 500–800 J could be done with the existing now Ti:Sa crystals of 20–30 cm diameter.

Two recently developed method of pulse shortening have been discussed in the subtitle 3. The ability to obtain a greatly broadened spectral bandwidth in Ti:Sa laser amplifiers was shown using both π- and σ-axis and shaping the spectral gain via engineering the spectral polarization of amplified pulses [34]. Amplification bandwidth exceeding 85 nm at a gain of 200 was demonstrated in a proof-of-principle experiment. These experiments have shown also that active pre-shaping of the pulse spectrum with PE amplification preceding saturated amplification in conventional CPA amplifiers can be successfully used to compensate the spectral red-shifting and gain narrowing that accompany amplification in Ti:Sa CPA systems. The computer modeling revealed that a polarization-encoded chirped pulse amplification scheme can be scaled to higher energies and produce multi-Joule pulses with bandwidth close to 200 nm, making few-cycle petawatt Ti:Sa systems feasible.

The multiple stage compression method based on spectral broadening using SPM in the bulk of material with the further recompression of the chirped pulse is able to deliver even shorter pulse duration below 10 fs without energy sacrificing [37]. Further development of this idea, with SPM in thin film below 1 mm and much higher intensity (up to tens of TW/cm^2) was

suggested [38]. Numerical simulations of two stage thin film compressor were done with the thicknesses of thin film elements 0.5 mm and 0.1 mm. The fundamental peak intensity after the first and second stages with temporal recompression procedure 16.6 and 43 TW/cm^2 at pulse durations 6.4 and 2.1 fs correspondingly are expected. This shortening of the pulse duration without energy losses allows to increase the output peak power to an additional order and achieve few hundred PW from the single channel of CPA laser systems.

The combination of EDP technique with TD Ti:Sa crystals for power amplifiers [39, 41, 43] also lets the ultra-high peak power amplifiers increase as well as the average power. In a proof-of-principle experiment, high-energy broadband amplification in a room temperature water-cooled EDP-TD head was demonstrated at a 10 Hz repetition rate instead of performing a traditional cryogenically cooled multipass scheme. Therefore, the limits associated with thermal effects and transverse amplified spontaneous emission can be overcome by the EDP-TD combination, enabling Ti:Sa laser systems to have a petawatt peak power and hundreds Hz repetition rates or kWs of average power.

Author details

Vladimir Chvykov

Address all correspondence to: VladimirChvykov@eli-alps.hu

ELI-Hu Nkft., Szeged, Hungary

References

[1] McClung F et al. Giant optical pulsations from ruby. Journal of Applied Physics. 1962;**33**(3):828

[2] Mocker W et al. Mode competition and self-locking effects in a Q-switched ruby laser. Applied Physics Letters. 1965;**7**:270

[3] Tajima T et al. Laser electron accelerator. Physical Review Letters. 1979;**43**:267

[4] Nicollas et al. Lasers and controlled thermonuclear fusion. Nature. 1972;**239**:1-29

[5] Available from: https://lasers.llnl.gov/about/nif [Internet]

[6] Available from:http://www-lmj.cea.fr/index.html [Internet]

[7] Damm T et al. Compression of picosecond pulses from a solid-state laser using self-phase modulation in graded-index fibers Optics Letters. 1985;**10**(4):176

[8] Strickland D et al. Compression of amplified chirped optical pulses. Optics Communication. 1985;**56**(3):219

[9] Giordmaine J et al. Compression of optical pulses. Journal of Quantum Electronics. 1968;**QE-4**:252

[10] Duguay M et al. Compression of pulses from a mode-locked He-Ne laser. Applied Physics Letters. 1969;**14**:14

[11] Treacy E. Optical pulse compression with diffraction gratings. IEEE Journal of Quantum Electronics. 1969;**5**(9):454

[12] Martinez O et al. Negative group-velocity dispersion using refraction. Journal of the Optical Society of America A. 1984;**1**(10):1003

[13] Moulton P. Spectroscopic and laser characteristics of Ti:Al2O3. Journal of the Optical Society of America B. 1986;**3**:125

[14] Taiha Joo, Yiwei Jia, Graham R. Fleming, Ti:sapphire regenerative amplifier for ultra-short high-power multikilohertz pulses without an external stretcher. Optics Letters. 1995;**20**:389

[15] Ian N. Ross et al. Generation of terawatt pulses by use of optical parametric chirped pulse amplification. Applied Optics. 2000;**39**(15):2422

[16] Ple F et al. Design and demonstration of a high-energy booster amplifier for a high-repetition rate petawatt class laser system. Optics Letters. 2007;**32**(3):238

[17] Gerstner. Extreme light. Nature. 2007;**446**:16

[18] Available from: http://www.eli-laser.eu [Internet]

[19] Yamakava K et al. Generation of 16-fs, 10-TW pulses at a 10-Hz repetition rate with efficient Ti:sapphire amplifiers. Optics Letters. 1998;**23**(7):525

[20] IshII N et al. Multimillijoule chirped parametric amplification of few-cycle pulses. Optics Letters. 2005;**30**(5):567

[21] Mourou G et al. Optics in the relativistic regime. Reviews of Modern Physics. 2006;**78**(2):309

[22] Speiser J. Scaling of thin-disk lasers—influence of amplified spontaneous emission. Journal of the Optical Society of America B: Optical Physics. 2009;**26**:26

[23] Peterson F et al. Suppression of parasitic lasing in large-aperture Ti:sapphire laser amplifiers. Optics Letters. 1999;**24**(14):963

[24] Bonlie J et al. Production of $>10^{21}$ W/cm^2 from a large-aperture. Ti:sapphire laser system. Applied Physics B. 2000;**70**:155

[25] Chvykov V et al. Transverse amplified spontaneous emission: the limiting factor for output energy of ultra-high power lasers. Optics Communication. 2014;**312**:216

[26] Koechner W. Solid State Laser Engineering. Berlin: Springer; 1996. p. 747

[27] Chvykov V et al. Suppression of parasitic lasing in multi-pass Ti-sapphire amplifiers, CWA34. In: Technical Digest CLEO. 2003

[28] Chvykov V et al. Large aperture multi-pass amplifiers for high peak power lasers. Optics Communication. 2012;**285**(8):2134

[29] Joyce D et al. Ti:sapphire laser crystals reach 200 mm diameter. Laser Focus World. 2010;**46**(3):37

[30] Chu Y et al. High-energy large-aperture Ti:sapphire amplifier for 5 PW laser pulses. Optics Letters. 2015;**40**(21):5011

[31] Yanovsky V et al. Ultra-high intensity-300-TW laser at 0.1 Hz repetition rate. Optics Express. 2008;**16**:2109

[32] Sung JH, Lee SK, Lee HW, Yoo JY, Nam CH. Development of 0.1 Hz 4.0 PW laser at CoReLS. In: Conference on Lasers and Electro-Optics, OSA Technical Digest (2016) (Optical Society of America, 2016), paper SM1M.3

[33] Chvykov V et al. Final EDP Ti:Sapphire amplifiers for ELI project. Proceedings of SPIE. 2015;9515 OJ. DOI: 10.1117/12.2182319

[34] Kalashnikov M et al. Polarization-encoded chirped pulse amplification in Ti:sapphire: A way toward few-cycle petawatt lasers. Optics Letters. 2016;**41**(1):25

[35] Claude Rolland, Corkum PB. Compression of high-power optical pulses. Journal of the Optical Society of America B. 1988;**5**:641

[36] Mevel E et al. Multielectron ionization processes in ultrastrong laser fields. Journal of the Optical Society of America B. 2003;**20**:105

[37] Chvykov V et al. Compression of ultra-high power laser pulses. CLEO-Proceeding. 2010: JThG4

[38] Mourou G et al. Single cycle thin film compressor opening the door to zeptosecond-exawatt physics. The European Physical Journal Special Topics. 2014;223(6):1181

[39] Chvykov V et al. Design of a thin disk amplifier with extraction during pumping for high peak and average power Ti:Sa systems (EDP-TD). Optics Express. 2016;**24**(4):3721

[40] Negel J, et al. 1.1 kW average output power from a thin-disk multipass amplifier for ultrashort laser pulses. Optics Letters. 2013;**38**:5442

[41] Chvykov V et al. High peak and average power Ti:sapphire thin disk amplifier with extraction during pumping. Optics Letters. 2016;**41**(13):3017

[42] Bahk S et al. Generation and characterization of the highest laser intensities 1022 W/cm2. Optics Letters. 2004;**29**:2837

[43] Nadymihaly R et al. Liquid-cooled Ti:Sapphire thin disk amplifiers for high average power 100-TW systems. Optics Express. 2017;**25**(6):6664